Pergamon

J. Appl. Maths Mechs, Vol. 59, No. 2, pp. 289–297, 1995

0021–8928/95 $24.00+0.00

0021–8928(95)00032-1

THE MECHANICS OF FATIGUE CRACK GROWTH IN A MEDIUM WITH MICRODAMAGE†

V. V. BOLOTIN and V. L. LEBEDEV

Moscow

(*Received* 24 *November* 1994)

Fatigue crack growth at a high stress level is considered using the model of a thin plastic zone taking microdamage accumulation in this zone into account. It is assumed that a crack grows when the stability condition of the "cracked body–loading" system is violated. This condition is treated in the framework of the principle of virtual work for systems with unilateral constraints. The damage accumulation process in the plastic zone and on its prolongation is assumed to depend on the opening stress range. The process of crack growth is studied by numerical simulation. Diagrams of the growth of fatigue cracks are obtained that describe all three stages of fatigue damage including the anomalous behaviour of short cracks and the accelerated growth near the final fracture. It is shown that the proposed theory predicts that the slope of the middle part of the diagram is close to two when the parameters of microdamage accumulation vary over a wide range.

The growth of fatigue cracks can be regarded as a result of a combination of two interacting phenomena: the transition of the "cracked body with load" system from one stable state into a neighbouring stable state, and the process of microdamage accumulation which occurs both in the tip zone and in the far field. From this point of view the mechanical model of the fatigue crack growth is based on a synthesis of fracture micro- and macromechanics [1, 2]. If the level of cyclic loading is sufficiently high, the fatigue crack growth is accompanied by plastic deformation. The growth rate then increases considerably, and the number of cycles until the final fracture occurs is reduced. In this case we speak of low-cycle fatigue (unlike the classical high-cycle fatigue). To describe the growth of classical fatigue cracks it is sufficient to combine linear fracture mechanics with one of the models of damage accumulation. In the case of low-cycle fatigue, to describe the phenomenon at the macroscopic level one needs to use one of the models of non-linear fracture mechanics [3–6]. In this paper we use the Leonov–Panasyuk–Dugdale model of a thin plastic zone.

1. Macroscopic cracks in common engineering materials are usually irreversible. This enables the "cracked body–load" system to be treated as a mechanical system with unilateral ideal constraints on the parameters which represent the dimensions of the cracks. It is natural to treat the behaviour of such systems using the principle of virtual work for systems with unilateral constraints [7]. It is then necessary to distinguish the usual generalized Lagrange coordinates, which describe the field of displacements in the body with fixed cracks, and the crack parameters, called generalized Griffith coordinates in [1]. Henceforth, for brevity, we will use the terms L-coordinates and G-coordinates, respectively.

We will assume that the number of G-coordinates $a_1, \ldots, a_m$ is finite, and their variations, compatible with the constraints, satisfy the inequalities

$$\delta a_j \geqslant 0, \quad j = 1, \ldots, m \tag{1.1}$$

Confining ourselves to quasistatic problems, we will write the condition of equilibrium of the "cracked body–load" system in the form

$$\delta A = \delta_L A + \delta_G A \leqslant 0 \tag{1.2}$$

where the work $\delta_L A$ is performed on variations of the L-coordinates while the work $\delta_G A$ is performed on variations of the G-coordinates. By definition [1, 2], all the adjacent positions must satisfy the condition $\delta_L A \equiv 0$ so that relation (1.2) reduces to the following

†*Prikl. Mat. Mekh.* Vol. 59, No. 2, pp. 307–317, 1995.

$$\delta_G A \leqslant 0 \tag{1.3}$$

We will call the state of the "cracked body–load" system a subequilibrium state [1] if $\delta_G A < 0$ for any permissible $\delta a_j > 0$, and an equilibrium state if $\delta_G A = 0$ for some of the variations $\delta a_j > 0$ and $\delta_G A < 0$ for the remaining variations. The equilibrium states can be stable, unstable or neutral depending on the behaviour of the system in the neighbourhood of an equilibrium state. If at least one variation $\delta a_j > 0$ exists for which $\delta_G A > 0$, the state is called a non-equilibrium state. It is obvious that this state is unstable. The corresponding theorems can be proved rigorously with certain limitations [8]. When $m = 1$ and for external potential forces this follows from energy considerations if we mean by variations in the dimensions of the crack δa_j the actual increment da.

In the case of cyclic loading it is necessary to take into account the dependence of the virtual work $\delta_G A$ on the loading prehistory, the growth of cracks, and the accumulation of plastic deformation and microdamage. A fatigue crack does not propagate when $\delta_G A < 0$ and grows continuously and $\delta_G A > 0$. $\delta_G (\delta_G A) < 0$. The second sign of the variation denotes that second-order terms are taken into account in the neighbourhood of the equilibrium state when conditions (1.1) are satisfied. The crack will grow intermittently if, at the instant when the equality $\delta_G A = 0$ is achieved, the condition $\delta_G (\delta_G A) < 0$ is not satisfied [9].

In order to formulate these conditions in terms of generalized forces we note that the work $\delta_G A$ is a linear form of the variation δa_j

$$\delta_G A \equiv \sum_{j=1}^{m} (G_j - \Gamma_j)\delta a_j \tag{1.4}$$

Here G_j are the active (moving) generalized forces, and Γ_j are the generalized resistance forces.

The division of the generalized forces into two classes is fairly arbitrary. As is usually done in fracture mechanics, we will relate the generalized resistance forces to the fracture work performed in the regions near the crack tips. Then, by linear fracture mechanics, the generalized forces G_j have the meaning of the strain energy release rates, while the generalized forces have the meaning of the corresponding critical values. Fatigue cracks do not grow when $G_j < \Gamma_j$ and begin to grow with respect to the generalized coordinate a_k when the equality $G_k = \Gamma_k$ is attained. In particular, if $m = 1$, the conditions for continuous crack growth have the form

$$G = \Gamma,\ dG/da < d\Gamma/da \tag{1.5}$$

where the subscripts have been omitted.

When the system becomes unstable, an abrupt increment in the crack by Δa occurs, after which the state of the system again becomes stable (a subequilibrium state). The increment Δa can be obtained from energy considerations. Neglecting all energy losses, apart from that which is due to the fracture work, we arrive at the equation

$$\int_a^{a+\Delta a} G(x)dx = \int_a^{a+\Delta a} \Gamma(x)dx \tag{1.6}$$

The x coordinate is measured along the direction of the assumed crack propagation.

2. A model of a thin plastic region was discussed in detail in [3–5]. We will consider the fundamental version of the model, namely, a plane opening mode crack in an unbounded plate subject to normal stresses σ_∞. We will denote the length of the crack by $2a$ and the length of the plastic zone by λ, and we will direct the coordinate axes as shown in Fig. 1. The faces of the crack at $|x| < a$ are stress-free. In the section $a < |x| < a + \lambda$ the normal stresses $\sigma_y(x)$ are, by definition, equal to the specified quantity σ_0, which is of the order of the yield stress of the material under tension and may be identical to it. Outside the plastic region, the thickness of which is assumed to be negligibly small, the material is linearly elastic with Young's modulus E. The solution of the mixed problem of the theory of elasticity reduces to the formula for the length λ of the plastic zone and the crack tip opening δ

$$\lambda = a(\sec\zeta - 1),\quad \delta = \frac{8\sigma_0 a}{\pi E}\ln\ \sec\zeta,\quad \zeta = \frac{\pi\sigma_\infty}{2\sigma_0} \tag{2.1}$$

Moreover, we will later need a formula for the normal displacement $\upsilon(x)$ when $a < |x| < a + \lambda$ and the normal stress $\sigma_y(x)$ when $|x| > a + \lambda$. These formulae may have different forms depending on the

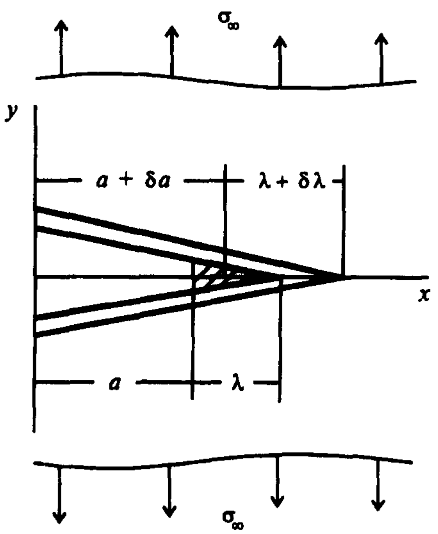

Fig. 1.

method by which they are obtained. Omitting the reference on the y coordinate, we will take the following expressions ($b = a + \lambda$)

$$v(x) = \frac{b\sigma_o}{\pi E}\left[\cos\theta \ln\frac{\sin^2(\zeta-\theta)}{\sin^2(\zeta+\theta)} + \cos\zeta \ln\frac{(\sin\zeta+\sin\theta)^2}{(\sin\zeta-\sin\theta)^2}\right]$$

$$\sigma_y(x) = f(a, b, x) \tag{2.2}$$

$$\theta = \text{arc}\ \cos\frac{x}{b},\quad f(a,\ b,\ x) = \frac{2\sigma_0}{\pi}\,\text{arc ctg}\left[\frac{a}{x}\left(\frac{x^2-b^2}{b^2-a^2}\right)^{1/2}\right]$$

To determine the active generalized force G we will use the relation

$$G\,\delta a = \delta_G A_e + \delta_G A_i \tag{2.3}$$

where $\delta_G A_e$ and $\delta_G A_i$ are the virtual works of the external and internal forces, respectively, calculated over the whole volume, including the tip zone. Since the material is assumed to be elastic outside the tip zone, variation of G-coordinates generates variations of the strain field outside the tip zone, which satisfy the conditions imposed on the variations of L-coordinates. This means [10] that the limits of the integration region can be transferred directly to the boundary of the tip zone. Unlike the similar discussions in the case of the J-integral, however, it is necessary to take two facts into account here. First, when the dimensions of the crack vary, the length of the end zone (2.1) will also undergo a variation (Fig. 1). Second, the boundary of the region may contract only up to the beginning of the varied tip zone, i.e. it is necessary to take into account in the calculations the work in the section $a + \lambda < |x| < a + \delta\lambda$. Hence, relation (2.3) takes the form

$$G = 2\sigma_0\delta a \int_a^{a+\lambda} \frac{\partial \upsilon}{\partial a}dx \tag{2.4}$$

Substituting the expression for $\upsilon(x)$ from (2.2) we obtain

$$G = G_0(\ln\ \cos\zeta + \zeta\,\text{tg}\,\zeta),\quad G_0 = \frac{8\sigma_0^2 a}{\pi E} \tag{2.5}$$

The details of the calculations were presented in [3] in the context of determining the specific work of fracture in the model of a thin tip zone, i.e. the generalized resistance force Γ. Since, when the crack starts to grow, $G = \Gamma$, the right-hand side of (2.5) is identical with the specific fracture work.

Note that the usual formula for the J-integral when choosing the contour of integration over the boundary of the tip zone has the form

$$J = -2\sigma_0 \delta a \int_a^{a+\lambda} \frac{\partial \upsilon}{\partial x} dx \tag{2.6}$$

The integral on the right-hand side is equal to $\delta/2$. Substituting δ from (2.1) here we obtain the well-known formula

$$J = G_0 \ln \sec \zeta \tag{2.7}$$

The results of calculations using Eqs (2.5) and (2.7) differ considerably particularly in the region of large σ_∞/σ_0. This is illustrated in Fig. 2, where curve 3 is drawn using Eq. (2.5) and curve 2 is drawn using Eq. (2.7). The difference between the right-hand sides of these formulas can be explained by their different origin: the generalized force G is obtained by considering the variation in the dimensions of the crack, whereas the J-integral corresponds to the "approach" of the body to a fixed crack. The product $G\,\delta a$ has the meaning of virtual work, whereas the product $J\,\delta a$, in general, does not allow of this interpretation. However, if the material of the body is everywhere elastic (not necessarily linearly), we can replace $\partial/\partial a$ by $-\partial/\partial x$ and vice versa in (2.4) and (2.6). In the model of the plastic zone, due to variation of its dimensions $\partial/\partial a \neq -\partial/\partial x$. For completeness, Fig. 2 shows a graph (curve 1) constructed from the formula of linear fracture mechanics $J = \pi\sigma_\infty^2 a/E$.

3. When calculating the generalized force one needs to take into account the inelastic nature of the deformation—the occurrence of residual stresses and strains, both ahead of the crack tip and behind this tip, cyclic hardening, and also the accumulation of microdamage in the tip zone and along its prolongation. Many factors are contradictory and do not always have an easily predictable effect. Thus, in addition to cyclic hardening, softening is also observed. Microdamage, accumulated ahead of a microscopic crack, reduces the specific fracture work but may also have the opposite effect.

We will now consider a simple analytical model, according to which the specific fracture work depends only on the opening at the crack tip $\delta \geqslant 0$ and a certain scalar microdamage measure $\psi \geqslant 0$. Then

$$\Gamma = \Gamma_0 f(\delta, \psi) \tag{3.1}$$

where Γ_0 is the specific fracture work for a "narrow" crack, in the undamaged material, while the function $f(\delta, \psi)$ satisfies the conditions $f(0, 0) = 1$, $\partial f/\partial \delta \geqslant 0$, $\partial f/\partial \psi \leqslant 0$. Under these conditions Eq. (3.1) enables one to describe the increase in the crack resistance due to plastic blunting of the crack and, to a certain extent, the effect of the prehistory.

Thus, for a short-term overload, δ increases, leading to an increase in the generalized force Γ and a delay in the crack growth. The introduction of a dependence on the measure ψ enables the reduction in the crack resistance due to the microdamage accumulation to be treated. To describe the latter along the extension of the crack $|x| \geqslant a$ we will introduce the scalar measure $\omega(x, N)$ which takes values in the interval $[0, 1]$. Then, the value $\omega = 0$ corresponds to an undamaged material, while $\omega = 1$ corresponds to a completely damaged material. It is obvious that

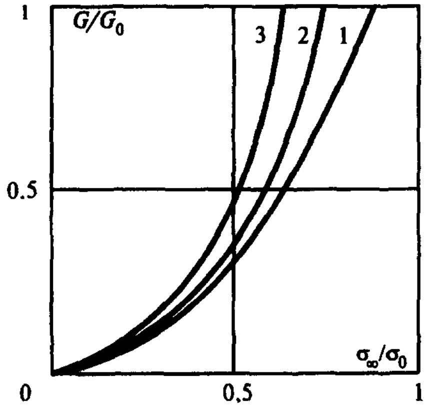

Fig. 2.

$$\psi(N) = \omega[a(N), N] \tag{3.2}$$

One of the simplest analytic representations for the right-hand side of (3.1) has the form

$$\Gamma = \Gamma_0[1 + (\delta/\delta_r)^{\beta}](1 - \psi^{\alpha}) \tag{3.3}$$

This formula, in addition to the specific work Γ_0 for the undamaged material, also contains three other parameters α, β, δ_r (the last of these has the dimensions of length). When $\beta > 0$, Eq. (3.3) describes the increase in the fracture toughness as the crack tip moves and as the stress level increases. Here δ is calculated from Eq. (2.1) by replacing σ_∞ by the maximum nominal stress of the cycle σ_∞^{max}. From the conditions, the crack propagates in the $y = 0$ plane, i.e. without kinking and branching, while outside the plastic zone the material remains elastic with the constant modulus E.

We will set up an equation for the microdamage measure $\omega(x, N)$. Here the problem arises as to which factor controls the microdamage accumulation: a cyclic change in the stresses or a cyclic change in the strains. In the first case the equation can be taken in the form

$$\partial\omega/\partial N = [(\Delta\sigma_y - \Delta\sigma_{th})/\sigma_f]^m \tag{3.4}$$

Here $\Delta\sigma_\infty$ is the range of the tensile stresses when $y = 0$. The parameters of the material $\sigma_f > 0$, $\sigma_{th} \geqslant 0$, $m > 0$ may depend on temperatures and other environmental conditions on the loading frequency, on the form of the cycle and, in particular, on the stress ratio $R = \sigma_\infty^{min}/\sigma_\infty^{max}$. The introduction of the threshold value $\Delta\sigma_{th}$ enables the so-called crack-closure effect [11] to be introduced into consideration.

In order to obtain the tensile stress range $\Delta\sigma_y$ it is sufficient to obtain the distribution of the tensile stresses for σ_∞^{max} and σ_∞^{min}. When $\sigma_\infty = \sigma_\infty^{max}$, Eq. (2.1) and the second formula of (2.2) give

$$\sigma_y^{max} = \begin{cases} \sigma_o, & a \leqslant |x| \leqslant a + \lambda \\ f(a, b, x), & |x| > a + \lambda \end{cases}$$
$$\lambda = a\left[\sec\left(\frac{\pi\sigma_\infty}{2\sigma_0}\right) - 1\right] \tag{3.5}$$

When unloading occurs down to $\sigma_\infty/\sigma_\infty^{min}$, residual stresses occur which are obtained by summing the stresses (3.5) with the stress corresponding to the nominal value of $\sigma_\infty^{min} - \sigma_\infty^{max}$ and the limit stress $2\sigma_0$. As a result, the stress range turns out to be

$$\Delta\sigma_y = \begin{cases} 2\sigma_0, & a \leqslant |x| \leqslant a + \lambda_p \\ 2f(a, b_p, x), & |x| > a + \lambda_p \end{cases}$$
$$\lambda_p = a\left[\sec\left(\frac{\pi\Delta\sigma_\infty}{4\sigma_0}\right) - 1\right], \quad b_p = a + \lambda_p \tag{3.6}$$

where $\Delta\sigma_\infty$ is the range of the nominal stresses.

Equations (3.5) and (3.6) are illustrated in Fig. 3. Curve 1 corresponds to a stress $\sigma_\infty/\sigma_\infty^{max}$, curve 2 corresponds to the residual stresses $\sigma_\infty/\sigma_\infty^{min}$, while curve 3 corresponds to the range $\Delta\sigma_y$. In Fig. 4 the ratio of the dimensions of the "internal" plastic zone λ_p to the dimensions λ is plotted versus the stress range $\Delta\sigma_\infty$ and the ratio $R = \sigma_\infty^{min}/\sigma_\infty^{max}$.

We will take the following as an alternative model of the accumulation of microdamage

$$\partial\omega / \partial N = \left\{\left[(\Delta\upsilon)^{1/2} - (\Delta\delta_{th})^{1/2}\right] / \delta_f^{1/2}\right\}^m \tag{3.7}$$

Here $\Delta\upsilon$ is the range of the relative normal displacement at the edge of the plastic zone, and δ_f, $\Delta\delta_{th}$ and m are parameters of the material, similar to the parameters from (3.4).

All the displacements occur in Eq. (3.7) under the square root sign. This is done so that a low stress level, i.e. when $\sigma_\infty^{min} \ll \sigma_0$, Eq. (3.7) can be used to describe classical (high-cycle) fatigue. In fact, for small values of σ_∞/σ_0 Eq. (2.1) and the second equation of (2.2) give displacements proportional to $\sigma_\infty^2 a$, i.e. proportional to the square of the stress intensity factor ΔK_I. Taking the square roots in (3.7)

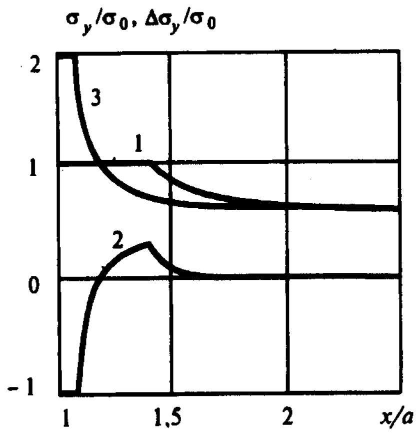

Fig. 3.

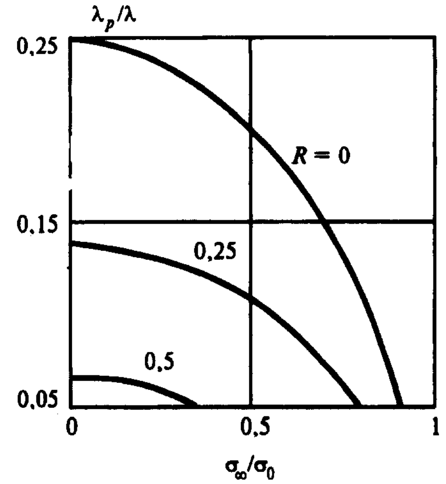

Fig. 4.

we ensure a threshold-power dependence of the damage accumulation rate on ΔK_{I} and, incidentally, the corresponding equation of the damage accumulation in Eq. (3.4). The choice between the models described by (3.4), (3.6) and (3.7) can only be made by comparing the results of a prediction of the crack growth with experimental data.

4. To calculate the growth of fatigue cracks we will now turn to relations (1.5) and (1.6). During the incubation stage, when microdamage accumulation occurs at the tip of a fixed crack, we have the relation $G < \Gamma$ when $a = a_0 = \text{const}$. Equation $G = \Gamma$ is first achieved for a certain $N = N_*$. The further behaviour of the crack depends on the distribution of the microdamage in the tip zone and also on the extent to which the plastic opening of the crack affects the resistance to its growth.

Two typical situations are shown in Fig. 5, where we illustrate how the generalized forces G and Γ change during the crack growth. Here the curves of Γ_s correspond to a monotonic increase in the load and the dimensions of the crack. They are essentially R-curves [3–5]. Point 1 on the graphs corresponds to the beginning of loading, point 2 corresponds to the onset of the crack growth when $N = N_*$, and point 3 corresponds to the final fracture when $N = N_{**}$. Figure 5 was drawn on the assumption that the microdamage at the crack tip decreases rapidly with depth into the tip zone, so that the crack growth occurs continuously when both conditions from (1.5) are satisfied. Figure 5(b) illustrates the intermittent growth of the crack. Due to microdamage, which occupies a region with dimensions at the order of λ_p, the state of the system when the equality $G = \Gamma$ is first attained is unstable: $dG/da > d\Gamma/da$. An increase in dimensions of the crack by Δa occurs, which can be found from condition (1.6). In the new position of the tip of the crack $G = \Gamma$, and the process is repeated once more. A typical situation is that, when there is microdamage described by Eq. (3.4), an intermittent growth of the crack occurs initially and, possibly, recommences before the final fracture due to a rapid increase in the dimensions λ and λ_p. If we take the model in the form (3.7), the crack growth becomes continuous.

For a numerical analysis it is best to take samples of the dimensions of the crack a in equal fairly small steps Δa. The calculation algorithm reduces to calculating the values of ψ corresponding to achieving the equality $G = \Gamma$ for the closest value $a + \Delta a$, and integrating Eq. (3.4) before the instant when the equality (3.2) is achieved. This gives the required number of cycles, after which the procedure is repeated.

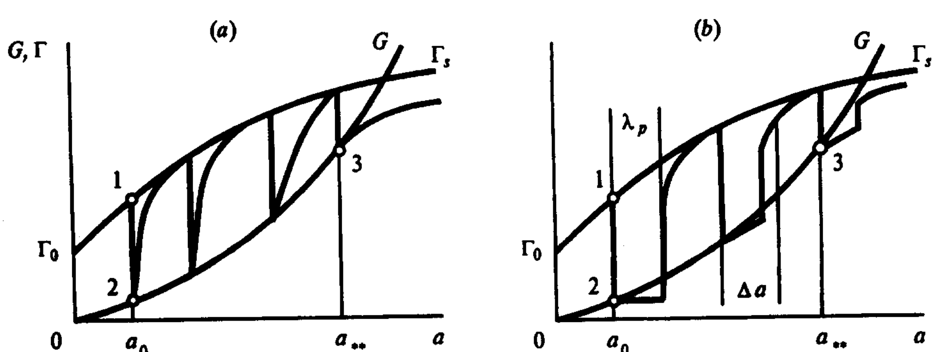

Fig. 5.

Calculations were carried out for the following numerical data: $E = 200$ GPa, $\sigma_0 = 500$ MPa, $\sigma_f = 5$ GPa, $\Delta\sigma_{th} = 250$ GPa, $\alpha = 1$ and $\delta_a \to \infty$. The initial value of the specific fracture work was taken as $\Gamma_0 = 18$ kJ/m^2, which, within the framework of linear fracture mechanics, corresponds to a fracture toughness $K_{IC} = 60$ MPa m$^{1/2}$. The calculations showed that at the beginning the crack propagates intermittently. A stage of continuous growth then begins at a somewhat slower rate. The velocity of the crack propagation then increases, approximately as a power law, with a considerable acceleration as it approaches the final fracture. These features agree with experimental data. They can be explained qualitatively by considering the distribution of the microdamage measure $\omega(x, N)$ at the tip of the moving crack (Fig. 6). Figure 6 was drawn for $a_0 = 1$ mm, $\sigma_\infty^{max} = 200$ MPa, and $\sigma_\infty^{min} = 0$. Curves 1–4 relate to the initial stage of growth. Curve 1 corresponds to $N = N_* = 42$ while curves 2–4 correspond to $n = 65$, 97, and 251 cycles. Curves 5 ($N = 1000$) and 6 ($N = 1170$) correspond to a later stage of crack growth. The projection of the left points of these curves onto the horizontal axis indicates the current dimensions of the crack $a(N)$. Until the crack begins to grow, i.e. $N < N_*$, considerable microdamage has accumulated in its tip zone (curve 1). This explains the intermittent growth of the crack at a relatively high rate. Later, due to the effect of the microdamage, accumulated in previous stages of the loading and in the far field, the growth becomes continuous. In the concluding stage the level of microdamage at the tip is reduced considerably.

The final result is of the greatest practical interest. This is represented by the diagram of the fatigue crack growth rate in which we have plotted the range of load parameters along the abscissa axis on a logarithmic scale, and the growth rate da/dN along the ordinate axis (also on a logarithmic scale). In Figs 7–9 we have chosen as the load parameters the range of the stress intensity factor ΔK_I, the range of the J-integral ΔJ, and the range of the generalized force ΔG, respectively. The graphs were drawn for the same data as above with the exception of the exponent in Eq. (3.4): it was taken to be $m = 4$. Curves 1–3 were drawn for the maximum stress of the cycle $\sigma_\infty^{max} = 150$, 200 and 300 MPa.

The form of the curves corresponds to the qualitative considerations presented above. The effect of the anomalous behaviour of the curves in the initial parts is noteworthy, and also their divergence as the crack continues to grow. This divergence is particularly great in Fig. 7, where we have taken the range of the stress intensity factor ΔK_I as the load parameter, as is usually done. On changing from ΔK_I to ΔJ (Fig. 8), the divergence between the curves decreases, although it still remains considerable. The closest arrangement of the curves is observed in Fig. 9. This serves as an indirect confirmation of the consistency of the proposed model. We can find another argument in favour of this model by considering the slope of the curves at their middle part. In Fig. 7 the slope factors (in double logarithmic coordinates) are equal to two (in Figs 8 and 9 they are close to unity). This agrees on the whole with experimental data on low-cycle fatigue, in particular, with the so-called Coffin–Manson equation and the related semi-empirical equations. The fact that these angular coefficients are independent of the exponent m in the equation for the accumulation of microdamage (3.4) is important. This is clearly shown on the diagrams of the growth of fatigue cracks (Fig. 10). For all three curves the slopes in the middle part of the diagram are close to two, although the crack growth rate has changed by two orders of magnitude. The result obtained can serve as a basis for choosing between the two models of the microdamage accumulation described by Eqs (3.4) and (3.7). In the second case the crack growth rate is extremely sensitive to the choice of m.

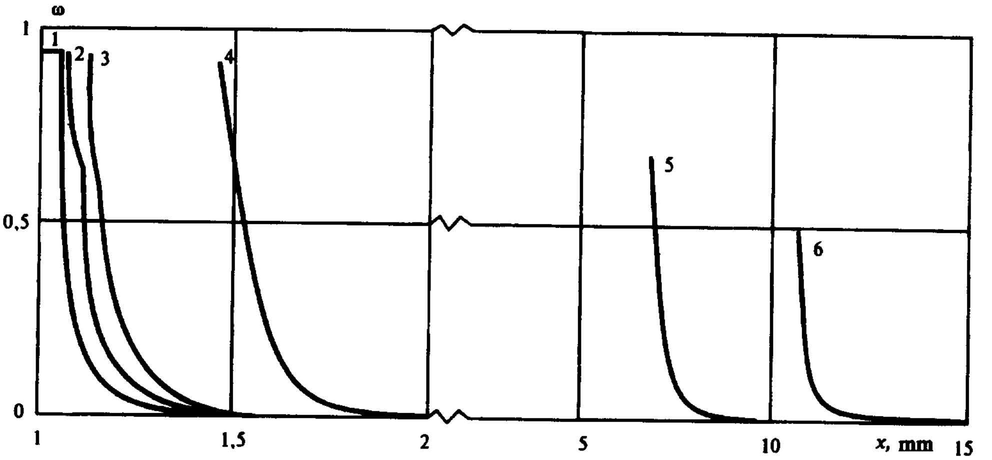

Fig. 6.

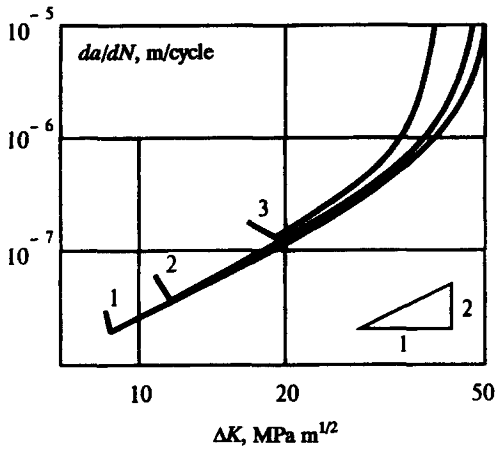

Fig. 7.

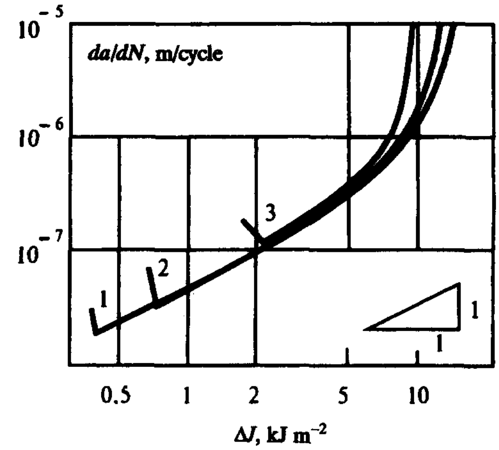

Fig. 8.

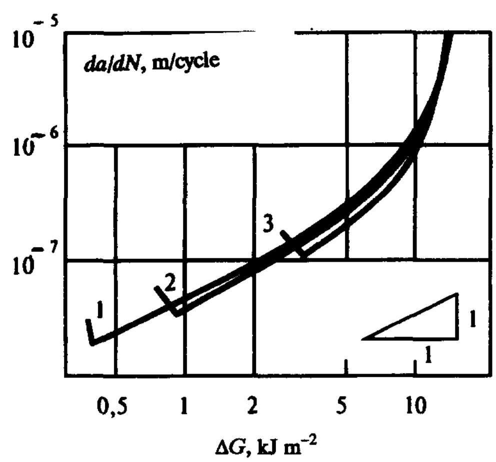

Fig. 9.

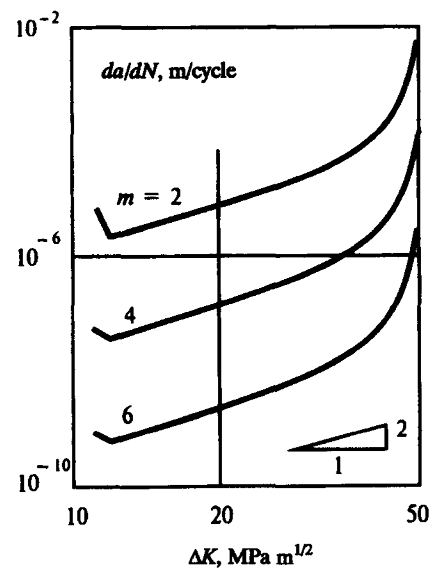

Fig. 10.

5. Certain qualitative conclusions which relate to the crack growth at the middle and concluding stages can be obtained using the quasistationary approximation [2]. We will represent the microdamage measure $\omega(x, N)$ in the form

$$\omega = \omega_{nf} + \omega_{ff} \tag{5.1}$$

Here $\omega_{nf}(x, N)$ is the measure of microdamage accumulated in the near field, or more accurately, in the internal tip zone with $a < |x| \leqslant a + \lambda_p$. The measure $\omega_{ff}(x\ N)$ includes microdamage in the far field, i.e. that which was accumulated before a particle of material enters the tip zone.

Suppose the dimensions of the tip zone λ_p are fairly small compared with the increment in the dimensions of the crack $a - a_0$ considered. Then, the crack growth rate can be assumed to be constant within the section ΔN, during which the crack tip travels a distance λ_p. Then

$$\Delta N \approx \lambda_p (da\,/\,dN)^{-1} \tag{5.2}$$

In the limits $a < |x| \leqslant a + \lambda_p$ the range of the tensile stresses is $2\sigma_0$. Hence, using Eq. (3.4), we obtain

$$\omega_{nf} \approx \lambda_p (da/dN)^{-1}[(2\sigma_0 - \Delta\sigma_{th})/\sigma_f]^m \tag{5.3}$$

Substituting (3.5), (3.2), (3.3), (5.1) and (5.3) into the condition $G = \Gamma$ we obtain the following approximate equation for the crack growth rate

$$\frac{da}{dN} \approx \lambda_p \left(\frac{2\sigma_0 - \Delta\sigma_{th}}{\sigma_f}\right)^m \left[\left(1 - \frac{G}{\Gamma_s}\right)^{1/\alpha} - \omega_{ff}(N)\right]^{-1} \tag{5.4}$$

Here, for brevity we have put $\Gamma_s = \Gamma_0[1 + (\delta/\delta_f)^\beta]$. For the middle stage of the crack growth $G \ll \Gamma_s$, $\omega_{ff}(x, N) \ll 1$. Taking into account the fact that when $\Delta\sigma_\infty/\sigma_0$ is sufficiently small

$$\lambda_p \approx \pi(\Delta\sigma_\infty)^2 a/(32E) \tag{5.5}$$

we obtain the growth rate da/dN proportional to the square of the stress intensity factor range ΔK_I, irrespective of the value of the exponent m in the initial equation (3.4). The last factor in (5.4) on the right-hand side describes the acceleration of the crack growth at the concluding stage.

We will carry out similar calculations as they apply to the simplified version of Eq. (3.7)

$$\partial\omega/\partial N = \left\{\left[(\Delta\delta)^{1/2} - (\Delta\delta_{th})^{1/2}\right]/\delta_f^{1/2}\right\}^m, \quad a \leqslant |x| \leqslant a + \lambda_p \tag{5.6}$$

where $\Delta\delta$ is the range of plastic tip opening displacement within the cycle.

For ω_{nf} and da/dN we obtain expressions similar to (5.3) and (5.4) when $[(2\sigma_0 - \Delta\sigma_{th})/\sigma_f]^m$ is replaced by the quantity on the right-hand side of Eq. (5.6).

Taking (2.2) and (5.5) into account we find that the growth rate da/dN when $G \ll \Gamma_s$, $\omega_{ff}(N) \ll 1$ is approximately proportional to $(\Delta K_I)^{m+2}$. The strong dependence of the crack growth rate on the exponent m shows that, of the two models of microdamage accumulation, we are inclined to choose the model described by Eq. (3.4).

This research was carried out with financial support from the Russian Foundation for Basic Research (93-013-1648) and the International Science Foundation (RLS000).

REFERENCES

1. BOLOTIN V. V., The equations of fatigue crack growth. *Izv. Akad. Nauk SSSR. MTT* 4, 153–160, 1983.
2. BOLOTIN V. V., A unified approach to damage accumulation and fatigue cracks growth. *Engng Fract. Mech.* **22**, 3, 387–398, 1985.
3. PARTON V. A. and MOROZON Ye. M., *The Mechanics of Elastoplastic Fracture*. Nauka, Moscow, 1985.
4. PLUVINAGE G., *The Mechanics of Elastoplastic Fracture*. Mir, Moscow, 1993.
5. WNUK M. P., Mathematical modelling of nonlinear phenomena in fracture mechanics. *Nonlinear Fracture Mechanics*, pp. 359–451. Springer, Vienna, 1990.
6. VAKULENKO A. A., MOROZOV N. F. and PROSKURA A. V., Evaluation of crack growth rate. *Fiz.-Khim. Mekh. Materialov* **29**, 3, 137–140, 1993.
7. BOLOTIN V. V., On the dynamic propagation of cracks. *Prikl. Mat. Mekh.* **56**, 1, 150–162, 1992.
8. IVANOV A. P., Stability of systems with holding constraints. *Prikl. Mat. Mekh.* **48**, 5, 725–732, 1984.
9. BOLOTIN V. V., Mechanics of fatigue fracture. *Nonlinear Fracture Mechanics*, pp. 1–59. Springer, Vienna, 1990.
10. BOLOTIN V. V., The stability and growth of cracks under non-potential loadings. *Izv. Akad. Nauk SSSR. MTT* 5, 148–157, 1987.
11. GOL'DSHTEIN R. V., ZHITNIKOV Yu. V. and MOROZOVA T. M., The equilibrium of a system of cuts taking their closure and opening into account. *Prikl. Mat. Mekh.* **55**, 4, 672–678, 1991.

Translated by R.C.G.